

MHD of Laboratory Plasmas: Crossovers with Astrophysics

Georgios Throumoulopoulos

*Section of Astro-geophysics, Department of Physics,
University of Ioannina*

The 5th Summer School of Hel.A.S.
“MHD in Astrophysics”
19 September 2024

Laboratory plasmas and Applications

- Gas discharges (gaseous electronics)
- Solid state plasmas (free electrons and holes in semiconductors)
- Plasma etching (surface cleansing)
- Safe and sustainable food production (decontamination, degradation of chemical residues of agricultural pesticides)
- Medicine and healthcare (medical applications, interaction with biological cells)
- Thrusters (spacecraft propulsion)
- Plasma accelerators (free-electron lasers, glass lasers)
- Controlled thermonuclear fusion

Astrophysical and Space plasmas

- Stars' cores and atmospheres
- Solar wind
- Interstellar plasmas
- Planets' magnetospheres
- Ionospheric plasma
- Auroras
- Neutron stars' magnetospheres
- Accretion disks
- Galactic plasmas

Plasma Physics

- Equilibrium
- Stability
- Dynamics, transport processes and turbulence
(There is experimental and theoretical evidence of an interplay between sheared zonal flows, Reynolds or residual stress, symmetry breaking, turbulence and transport regulation.)
- Plasma heating and current drive
- Dynamo effect (creation of magnetic fields)

Plasma models

- Kinetic theory

Boltzmann equation for particle species j :

$$\frac{\partial f_j}{\partial t} + \mathbf{v} \cdot \frac{\partial f_j}{\partial \mathbf{r}} + \frac{q_j}{m_j} \left(\mathbf{E} + \frac{\mathbf{v} \times \mathbf{B}}{c} \right) \cdot \frac{\partial f_j}{\partial \mathbf{v}} = \left(\frac{\partial f_j}{\partial t} \right)_{col.}$$

Ion-electron Coulomb collision frequency : $\nu_{ei} \propto T_e^{-3/2}$

For $kT \geq 1\text{KeV} \Rightarrow (\partial f_j / \partial t)_{col} \approx 0$

$$\text{Vlasov eq. : } \frac{\partial f_j}{\partial t} + \mathbf{v} \cdot \frac{\partial f_j}{\partial \mathbf{r}} + \frac{q_j}{m_j} \left(\mathbf{E} + \frac{\mathbf{v} \times \mathbf{B}}{c} \right) \cdot \frac{\partial f_j}{\partial \mathbf{v}} = 0$$

- Hybrid kinetic-fluid models
- Multi fluid models
- Magnetohydrodynamics (MHD)

Outline

- MHD: Introduction
- Thermonuclear Fusion
- Equilibrium and Relaxation
- Linear stability
- Summary

Magnetohydrodynamics (non-relativistic)

Priest, 1982; Goedblood & Poedts, 2004; Freidberg, 2014

$m_e/m_i \rightarrow 0$ (massless electrons), \mathbf{v} : ion fluid velocity, quasineutrality

$$\text{mass evolution: } \frac{D\rho}{Dt} = \frac{\partial\rho}{\partial t} + \nabla \cdot (\rho\mathbf{v}) = 0 \quad (1)$$

$$\text{momentum evolution: } \rho \frac{D\mathbf{v}}{Dt} - \mathbf{j} \times \mathbf{B} + \nabla P - \rho\mathbf{g} = 0 \quad (2)$$

$$\text{energy evolution: } \frac{DP}{Dt} + \gamma P \nabla \cdot \mathbf{v} = 0 \quad (3)$$

$$\nabla \cdot \mathbf{B} = 0 \quad (4)$$

$$\nabla \times \mathbf{B} = \mu_0 \mathbf{j} \quad (5)$$

$$\text{Ohm's and Faraday's laws: } \frac{\partial \mathbf{B}}{\partial t} = \nabla \times [\mathbf{v} \times \mathbf{B} - \eta \mathbf{j}] \quad (6)$$

$$\frac{D}{Dt} \equiv \frac{\partial}{\partial t} + \mathbf{v} \cdot \nabla : \text{Lagrangian (convective) derivative}$$

Ideal versus resistive MHD

From (5) and (6) \Rightarrow

$$\frac{\partial \mathbf{B}}{\partial t} = \nabla \times (\mathbf{v} \times \mathbf{B}) + \frac{\eta}{\mu_0} \nabla^2 \mathbf{B} \quad (7)$$

Magnetic Reynolds number:

$$R_m = \left| \frac{\nabla \times (\mathbf{v} \times \mathbf{B})}{(\eta/\mu_0) \nabla^2 \mathbf{B}} \right| \sim \frac{\mu_0 v_A L}{\eta}$$

$$L = \left| \frac{\mathbf{B}}{\nabla B} \right|, \quad \mathbf{v} \sim v_A = \frac{B}{(\mu_0 \rho)^{1/2}} : \text{Alfvén velocity}$$

- Ideal MHD ($R_m \gg 1$): The plasma elements “are frozen” into the magnetic field lines.
- Resistive MHD ($R_m \leq 1$): As R_m gets lower values the motion of the plasma elements gradually decouples from that of the magnetic field lines.

Resistive MHD

The induction equation (6) for $R_m \ll 1$ becomes a diffusion equation:

$$\frac{\partial \mathbf{B}}{\partial t} = \frac{\eta}{\mu_0} \nabla^2 \mathbf{B} \quad (8)$$

Rough estimate of the solution of (8) [$\nabla^2 \mathbf{B} \approx \mathbf{B}/L^2$]:

$$\frac{\partial \mathbf{B}}{\partial t} = \frac{\eta}{\mu_0 L^2} \mathbf{B} \Rightarrow \mathbf{B} = \mathbf{B}_0 \exp\left(-\frac{t}{\tau_R}\right)$$

$\tau_R \equiv \mu_0 L^2 / \eta$: resistive skin time

- Characteristic time for magnetic field penetration into a plasma (or external conductor).
- It can also be interpreted as the time for annihilation of the magnetic field; as the field lines move through the plasma, the induced currents cause Ohmic heating of the plasma.

Ideal MHD

The induction equation (6) reduces to

$$\frac{\partial \mathbf{B}}{\partial t} = \nabla \times (\mathbf{v} \times \mathbf{B}) \quad (9)$$

- Eq. (9) has the consequence of the magnetic lines “frozen” into the plasma.

$\tau_A \equiv L/v_A$ = Alfvén transit time: characteristic time scale for the ideal MHD effects.

$$R_m = \frac{\tau_R}{\tau_A} \approx 10^6 \text{ for sun and tokamak plasmas} \Rightarrow$$

two different time scales

- fast ideal-MHD time scale τ_A
- slow resistive-MHD time scale τ_R

Since $R_m \gg 1$ for a wide range of laboratory and astrophysical plasmas, ideal MHD is appropriate for describing such plasmas.

Ideal MHD scale independence

Reference quantities:

$$l_0, B_0, \rho_0, \quad v_0 = v_{A,0} = B_0 / \sqrt{\mu_0 \rho_0} \rightarrow t_0 = l_0 / v_0$$

Basic reference quantities: l_0, B_0, t_0

Dimensionless dependent variables:

$$\tilde{\rho} = \rho / \rho_0, \quad \tilde{\mathbf{v}} = \mathbf{v} / v_0, \quad \tilde{P} = P / (B_0^2 / \mu_0), \quad \tilde{\mathbf{B}} = \mathbf{B} / B_0, \quad \tilde{\mathbf{g}} = (l_0 / v_0^2) \mathbf{g}$$

Dimensionless ideal MHD **not dependent on l_0, B_0, ρ_0** (omitting tildes):

$$\frac{\partial \rho}{\partial t} + \nabla \cdot (\rho \mathbf{v}) = 0 \quad (10)$$

$$\rho \left(\frac{\partial \mathbf{v}}{\partial t} + \mathbf{v} \cdot \nabla \mathbf{v} \right) - (\nabla \times \mathbf{B}) \times \mathbf{B} + \nabla P - \rho \mathbf{g} = 0 \quad (11)$$

$$\frac{\partial P}{\partial t} + \mathbf{v} \cdot \nabla P + \gamma P \nabla \cdot \mathbf{v} = 0 \quad (12)$$

$$\frac{\partial \mathbf{B}}{\partial t} - \nabla \times (\mathbf{v} \times \mathbf{B}) = 0, \quad \nabla \cdot \mathbf{B} = 0 \quad (13)$$

Scales of different plasmas

Basic reference quantities	l_0 (m)	B_0 (T)	t_0 (s)
Tokamak	10	5	3×10^{-6}
Earth magnetosphere	4×10^7	3×10^{-5}	6
Solar coronal loop	10^8	3×10^{-2}	15
Neutron star magnetosphere	10^6	10^8	10^{-2}
Accretion disk YSO	1.5×10^9	10^{-4}	7×10^5
Accretion disk AGN	4×10^{18}	10^{-4}	2×10^{12}
Galactic plasma	10^{21}	10^{-8}	10^{15}

The dimensionless ideal MHD equations do not depend on the plasma size, l_0 , on the magnitude of the magnetic field, B_0 , and on the density, ρ_0 , i.e. on the time scale, t_0 . This provides the basis for the description of macroscopic dynamics of a large portion of matter in the Universe and, hence, for effective cross-fertilization between laboratory and astrophysical plasma physics.

MHD region of validity

Underlying conditions: (1) *high collisionality*

(2) *small ion gyro radius* (3) *small resistivity*

Conditions (2) and (3) are well satisfied in high-temperature plasmas but, in contrast, condition (1) is never satisfied:

Ion-electron Coulomb collision frequency: $\nu_{ei} = \frac{ne^2}{m_e} \eta$

electrical resistivity : $\eta \propto T_e^{-3/2}$

Despite of that:

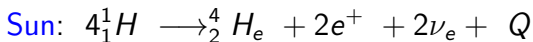
- In a magnetized plasma the magnetic field can play the role of collisions because of the particle gyro-motion (mean-free path \approx Larmor radius). For this reason MHD is particularly relevant to the physics perpendicular to \mathbf{B} .
- However, several important phenomena, such as Landau damping and those associated with energetic particles, require more fundamental models.

Outline

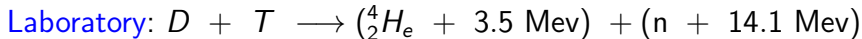
- MHD: Introduction
- **Thermonuclear Fusion**
- Equilibrium and Relaxation
- Linear stability
- Summary

Thermonuclear Fusion

Fusion occurs in the center of stars, e.g. in the center of the Sun in a fully ionized hydrogen plasma.



$$4 \cdot 10^9 \text{ kgr/sec} \implies 4 \times 10^{26} \text{ Watt}$$



Lawson condition [Wesson, 2004]: To produce more energy by fusion reactions than that required to heat the plasma and compensate the radiation losses:

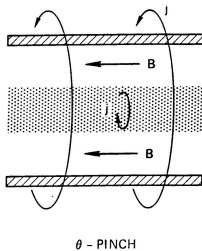
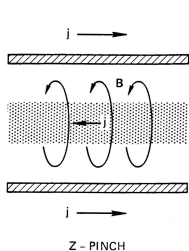
$$n \tau_E T \geq 10^{21} \text{ m}^{-3} \text{ sec KeV}, \quad T_i \approx T_e = T \approx 10 \text{ KeV}, \quad n_D \approx n_T = n/2$$

τ_E : energy confinement time (energy transport $\propto (3/2)nT/\tau_E$)

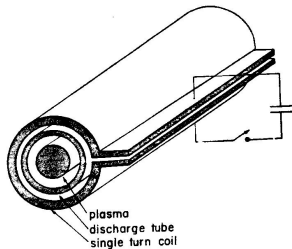
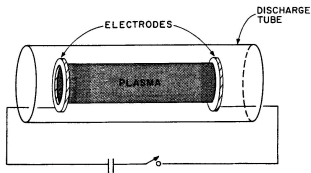
• Magnetic confinement: $n \approx 10^{21} \text{ m}^{-3}$, $\tau_E \approx 0.1 \text{ sec}$

• Inertial confinement: $n \approx 10^{31} \text{ m}^{-3}$, $\tau_E \approx 10^{-11} \text{ sec}$

The first experiments (pinches)



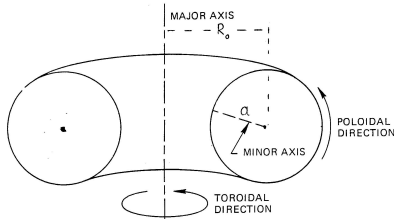
$$\text{Equilibrium: } \mathbf{j} \times \mathbf{B} - \nabla P = 0$$



Schematic diagrams of z-pinch (left) and θ -pinch (right) devices

Toroidal equilibrium requirements

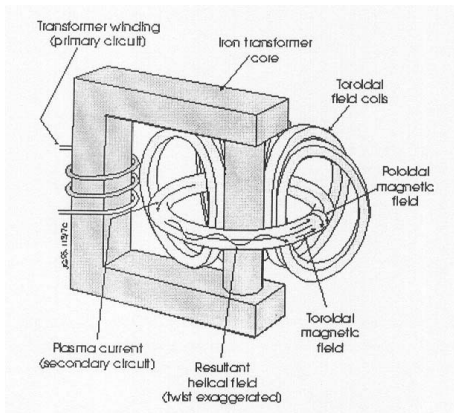
- 1 Any MHD equilibrium must be supported by externally supplied currents; it is not possible to create a configuration confined solely by the currents flowing within the plasma itself (consequence of the Virial theorem [Shafranov, 1966; Freidberg, 2014]).



Toroidal geometry

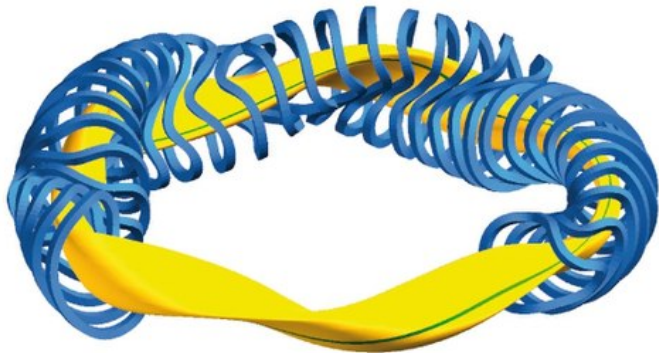
- 2 A **toroidal** equilibrium can not be established by a purely toroidal magnetic field; to confine the plasma a **poloidal** component B_p is necessary.

Tokamak



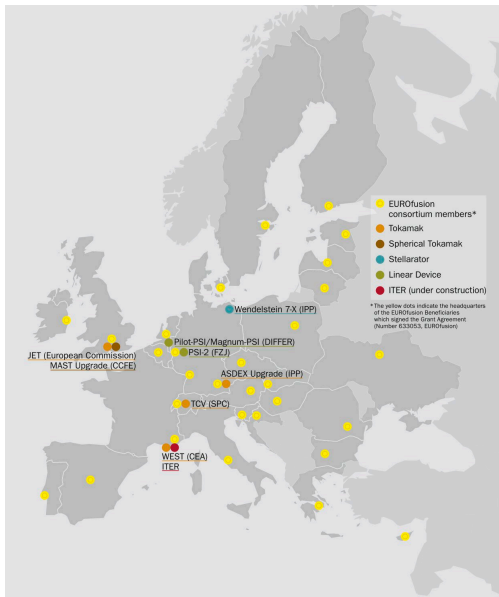
In a tokamak, the toroidal field component B_t is produced by external coils, while the poloidal component B_p is produced by a large toroidal plasma current induced by a transformer.

Stellarator



In a stellarator, the helical magnetic field is entirely produced by currents of external coils.

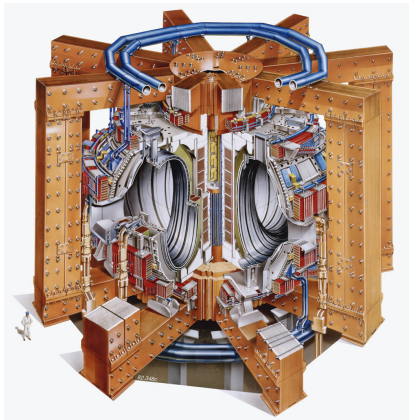
The European Fusion Program



The National Program for Controlled Thermonuclear Fusion

- National Centre For Scientific Research Demokritos
- National Technical University of Athens
- Foundation for Research and Technology - Hellas
- The University of Ioannina
- National and Kapodistrian University of Athens
- University of Thessaly
- Aristotle University of Thessaloniki
- Technical University of Crete
- Hellenic Mediterranean University
- University of Patras

The Joint European Torus (1)



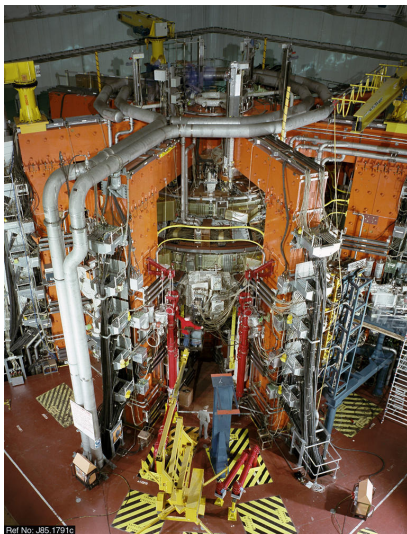
Cutaway diagram of the JET torus (with man for scale)

Geometric and operational figures

$$R_0 = 2.96 \text{ m}, \quad a = 1.25 \text{ m}, \quad b = 2.10 \text{ m}$$

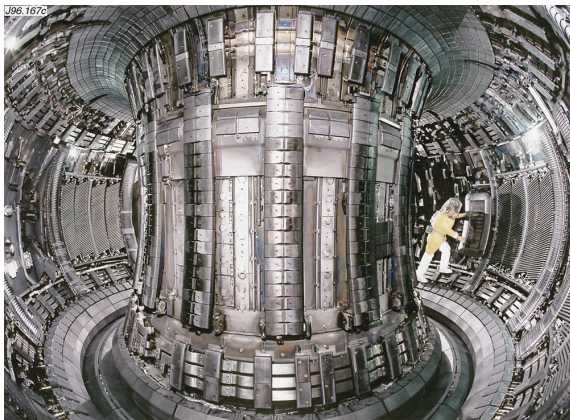
$$B_t = 3.45 \text{ T}, \quad B_p \approx 10^{-1} B_t, \quad I_t = 3.2 - 4.8 \text{ MA}$$

The Joint European Torus (2)



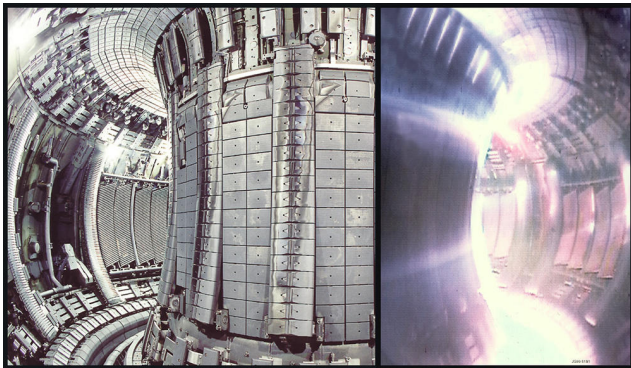
The JET machine during the 1985 construction phase

The Joint European Torus (3)



Taken in 1996, this is a wide angle view inside the torus showing a man wearing protective clothing performing maintenance within the vessel.

The Joint European Torus (4)



A split image of the inside of the torus, showing the plasma.)

Results: $nT_E T \approx 0.65 \times 10^{21} \text{ m}^{-3} \text{ sec Kev}$

Lawson condition: $nT_E T \geq 10^{21} \text{ m}^{-3} \text{ sec Kev}$

Results of D-T discharges at JET

- 1997: Fusion Gain record at a pulse of 3 sec
[Thomas et al, PRL (1998)]:

$$\text{Fusion Gain } Q = \frac{\text{Fusion energy}}{\text{Absorbed energy}} = 0.65$$

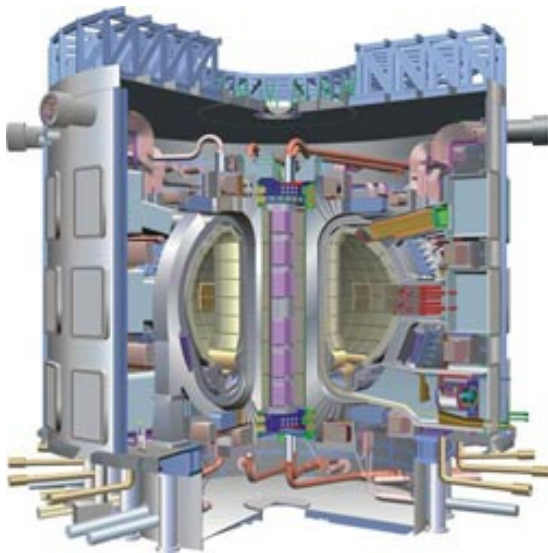
Fusion energy produced: $E_f=30.15$ MJ

- 2021: Fusion Energy record at a pulse of 5 sec:

$$E_f=59 \text{ MJ}$$

$$Q=0.33$$

The next step: ITER



International Thermonuclear Experimental Reactor

The ITER project

- 1 Partners: European Union (with Switzerland), Japan, Russia, China, USA, India, South Korea
- 2 Goal: Feasibility of controlled fusion for electric power production
- 3 Site: Cadarache, France
- 4 Budget: 25×10^9 Euros
- 5 Fusion power: 400 MW
- 6 $\frac{\text{Output power}}{\text{Input power}} = 10$

The site of under construction ITER



ITER: The under construction plasma chamber



Outline

- MHD: Introduction
- Thermonuclear Fusion
- Equilibrium and Relaxation
- Linear stability
- Summary

Ideal MHD equilibrium equations

$$\nabla \cdot (\rho \mathbf{v}) = 0 \quad (14)$$

$$\rho(\mathbf{v} \cdot \nabla)\mathbf{v} - \mathbf{j} \times \mathbf{B} + \nabla P - \rho \mathbf{g} = 0 \quad (15)$$

$$\nabla \cdot \mathbf{B} = 0 \quad (16)$$

$$\nabla \times \mathbf{B} = \mathbf{j} \quad (17)$$

$$\nabla \times \mathbf{E} = 0 \Rightarrow \mathbf{E} = -\nabla\Phi \quad (18)$$

$$-\nabla\Phi + \mathbf{v} \times \mathbf{B} = 0 \quad (19)$$

In addition, an “equation of state” usually in connection with either isentropic processes or isothermal processes or incompressibility.

Equilibrium with linear velocity: $(\mathbf{v} \cdot \nabla)\mathbf{v} = 0$

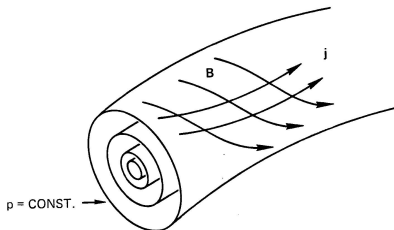
Equilibrium characteristics

$$(\mathbf{v} \cdot \nabla)\mathbf{v} = \mathbf{g} = 0, \quad \mathbf{j} \times \mathbf{B} = \nabla P \quad (20)$$

$$\mathbf{B} \cdot \nabla P = 0, \quad \mathbf{j} \cdot \nabla P = 0$$

Diamagnetic current:

$$\mathbf{j}_{\perp} = \frac{\mathbf{B} \times \nabla P}{B^2} \stackrel{\tau = \text{const.}}{=} T \frac{\mathbf{B} \times \nabla n}{B^2}$$



The magnetic surfaces, which \mathbf{B} lies on, the currents surfaces and the isobaric surfaces ($P = \text{const.}$) are common.

Existence of nested, toroidal magnetic surfaces

- A set of such well defined surfaces is guaranteed in 2D systems (translationally symmetric, axisymmetric as the tokamak, and helically symmetric).
- It is questionable in generic 3D geometry because of the magnetic field braiding [Grad, 1967; Stix, 1973].
- For this reason, plasma confinement in stellarators requires certain kind of **quasisymmetry**, e.g. 2D dependence of the magnetic field modulus in certain system of coordinates [Helander, 2014].

Grad-Shafranov equation

Cylindrical coordinates (z, R, ϕ)

Axisymmetry: $\forall A \quad \partial A / \partial \phi = 0$

Linear velocity, $\mathbf{g} = 0$

$$\Delta^* \psi(R, z) + \frac{1}{2} \frac{dI^2}{d\psi} + R^2 \frac{dP}{d\psi} = 0, \quad \Delta^* \equiv \frac{\partial}{\partial R^2} - \frac{1}{R} \frac{\partial}{\partial R} + \frac{\partial}{\partial z^2} \quad (21)$$

- The poloidal magnetic flux-function $\psi(R, z)$ labels the magnetic surfaces.
- The pressure $P(\psi)$ and the poloidal current $I(\psi)$ are free functions.

Solovév solution

Linearizing ansatz: $P'(\psi) = -|P'| = \text{const.} \Rightarrow$

$$P = P_a - |P'|\psi, \quad \psi \geq 0, \quad \psi_a = 0,$$

The subscripts a and b indicate values on the magnetic axis and the plasma surface (boundary), respectively.

At the surface: $P_b = P_a - |P'|\psi_{\text{max}} = 0$

$$I I' = \frac{1}{2}(I^2)' = \epsilon \frac{|P'|}{(1 + \delta^2)}$$

$\epsilon = 0$: vacuum toroidal field, $B_\phi = I_0/R$, $I_0 = \text{const.}$

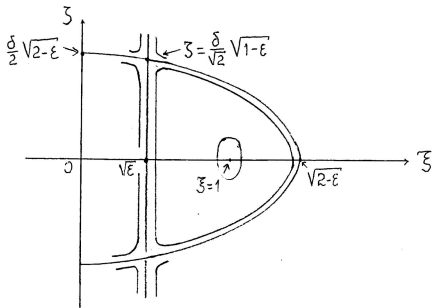
$\epsilon > 0$: diamagnetic plasma

$\epsilon < 0$: paramagnetic plasma

$$\text{Solution: } \psi = \left[\zeta^2(\xi^2 - \epsilon) + \frac{\delta^2}{4}(\xi^2 - 1)^2 \right] \frac{R_a^4 |P'|}{2(1 + \delta^2)} \quad (22)$$

$$\zeta = z/R_a, \quad \xi = R/R_a, \quad (I_0 = R_a)$$

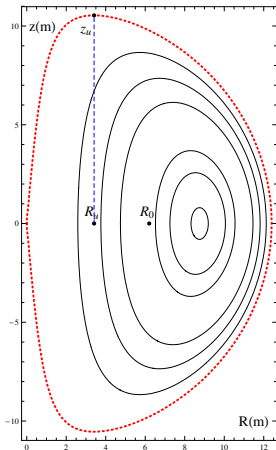
Diamagnetic Solovév equilibrium ($\epsilon \geq 0$)



- The configuration spontaneously exhibits an up-down symmetric separatrix containing a couple of X-points located at:
 $(\xi = \sqrt{\epsilon}, \zeta = \pm(\delta/\sqrt{2})\sqrt{1-\epsilon})$.
- For $\epsilon > 0$ the solution describes a tokamak equilibrium widely employed in the literature.
- For $\epsilon = 0$ the inner part of the separatrix touches the axis of symmetry and the equilibrium describes a spheromak.

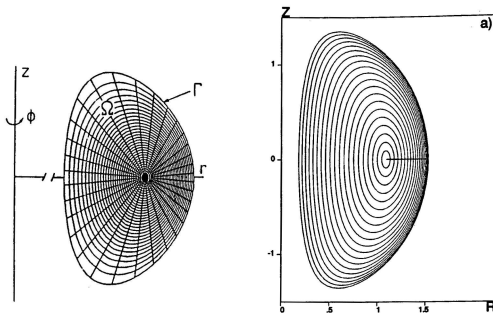
Paramagnetic Solovév equilibrium ($\epsilon < 0$)

[Arapoglou et al., 2013]



For $\epsilon < 0$ the separatrix touches the axis of symmetry at a single X-point located at $(R = 0, z = 0)$.

Numerical solutions of the GS equation



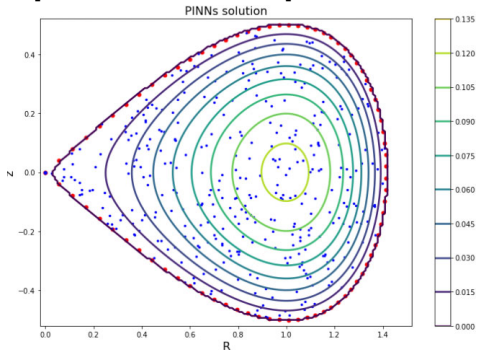
Solution for JET [Albanese et al., 1986] (left)

Comparison of a diamagnetic Solovév equilibrium with an (indistinguishable) numerical solution [Zakharov and Pletzer, 1999] (right).

Codes: PROTEUS, HELENA, extensions of HELENA to include plasma flow and pressure anisotropy [Poulipoulis et al., 2016; 2021].

Modeling Sun's corona employing the paramagnetic Solovév equilibrium

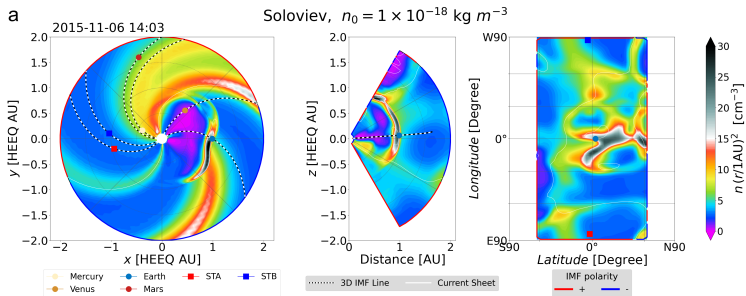
“Modelling solar coronal magnetic fields with physics-informed neural networks” [Baty & Vigon, 2024]



Equilibrium magnetic field lines (iso-contours of ψ) obtained with PINNs solver for the Solovév drop-shaped (paramagnetic) equilibrium [From Baty & Vigon].

Modeling CME employing the paramagnetic Solovév equilibrium

“Toroidal Miller-Turner and Solovév coronal mass ejection models in EUHFORIA” [Linan et al., 2024]



Distribution of scaled mass density at the moment of arrival at Earth as a function of the initial CME density, n_0 , simulated with the (paramagnetic) Solovév CME model [from Linan et al.].

Force-free equilibrium states

$$\mathbf{j} = \nabla \times \mathbf{B} = 0 \Rightarrow \mathbf{B} = \nabla Y \text{ or } \mathbf{j} \parallel \mathbf{B} \ (\mathbf{j} \times \mathbf{B} = 0), \quad -\nabla P + \rho \mathbf{g} = 0$$

In many cases in the astrophysical and laboratory plasmas flow very large currents. Then, the respective magnetic forces would be too strong to be balanced by pressure-gradient, gravitational and inertial forces. Therefore, the current density tends to be parallel to the magnetic field.

$$\nabla \times \mathbf{B} = \lambda \mathbf{B} \quad (23)$$

- Linear force-free states (LFF): $\lambda = \text{constant}$

$$\text{Then : } \nabla^2 \mathbf{B} = \lambda \mathbf{B}, \quad \nabla^2 : \text{Laplace operator} \quad (24)$$

- Non-linear force-free states (NLFF): $\lambda = \lambda(\mathbf{x})$

In Sun's chromosphere and corona LFF fields is a satisfactory approximation while in the photosphere NLFF ones are preferable [Wiegelmann & Sakurai, 2021].

Woltjer-Taylor relaxation

- **Taylor's conjecture**: In the presence of resistivity, however small, breaking the local conservation of magnetic helicity, the global (throughout the plasma volume) magnetic helicity remains invariant [Taylor, 1974].
- Minimization of the magnetic energy under the **single constraint of global magnetic helicity**, produces LFF states.
- For axisymmetric systems those states satisfy the following form of the Grad-Shafranov equation:

$$\Delta^* \psi + \lambda^2 \psi = 0 \quad (25)$$

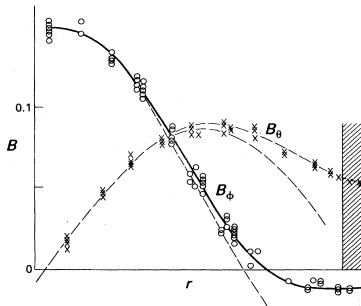
- The respective equation for translationally symmetric systems is

$$\nabla^2 \psi + \lambda^2 \psi = 0, \quad \nabla^2 : \text{2D Laplace operator} \quad (26)$$

Reversed-field-pinch relaxed states

For a circular-cross-section “torus” of large-aspect ratio we may take the cylindrical limit in which the 1D LFF well-known “Bessel function” solution is

$$B_r = 0, \quad B_\theta = \alpha J_1(\lambda r), \quad B_z = \alpha J_0(\lambda r), \quad \alpha : \text{minor radius}$$



Experimental and theoretical magnetic field profiles, HBTX-1A machine, Culham [from Bodin, 1984].

Spheromak relaxed states

Eigenvalue problem: $\Delta^* \psi_i + \lambda_i^2 \psi_i = 0$, $\psi_i = 0$ on the boundary (27)

Axisymmetric solution for an orthogonal cross section of height h and radius α [Bondeson et al., 1981; Finn et al., 1981]:

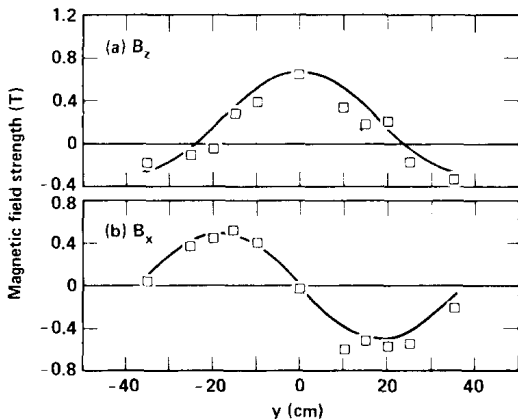
$$\text{Lowest eigenvalue : } \lambda = \left[\left(\frac{3.83}{\alpha} \right)^2 + \left(\frac{\pi}{h} \right)^2 \right]^{1/2}, \quad \frac{h}{\alpha} \leq 1.67 \quad (28)$$

$$\begin{aligned} B_R &= -B_0 k J_1(IR) \cos(kz) \\ B_z &= B_0 k J_0(IR) \sin(kz) \\ B_\phi &= B_0 \lambda J_1(IR) \sin(kz) \end{aligned} \quad (29)$$

$kh = \pi$, $l\alpha = 3.83$, (R, ϕ, z) cylindrical coordinates

For $h/a > 1.67$ the relaxed state becomes nonaxisymmetric.

Comparison with the BETA II spheromak, LLNL



Experimental and theoretical (solution (29)) profiles of the magnetic field on the mid-plane $z = 0$ in the BETA II spheromak at LLNL. (a) poloidal field B_z ; (b) toroidal field B_ϕ [from Turner et al., 1983].

Constructing 3D Sun LFF fields

$$\nabla^2 \mathbf{B} = \lambda \mathbf{B}, \quad \lambda = \text{const.}, \quad \nabla^2 = \frac{\partial^2}{\partial x^2} + \frac{\partial^2}{\partial y^2} + \frac{\partial^2}{\partial z^2}$$

Cartesian coordinates (x, y, z) with z corresponding to the height from the Sun surface.

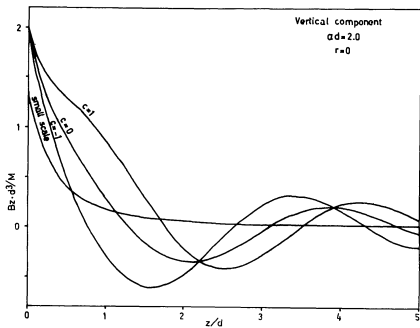
Methods of construction

- Green functions [Chiu & Hilton, 1977]
- Separation of variables [Seehafer, 1978]
- Fourier transforms [Alissandrakis, 1981]

λ in general is approximated by observations.

These methods can also be used to compute a potential field ($\lambda = 0$).

Construction of Sun's upper atmosphere 3D LFF fields by Fourier transforms



The vertical component, B_z , of a force-free field as a function of height. The computation was performed using as boundary condition the z component of a dipole field placed vertically at height d below the boundary, with $\lambda d = 2$. Three curves for different values of the parameter C are presented, parameter relating to the vertical derivative of B_z at the boundary [from Alissandrakis, 1981].

An axisymmetric NLFF equilibrium (1)

[Low & Lou, 1990]

$$\Delta^* \psi + \lambda I(\psi) = 0, \quad \lambda = \frac{dl}{d\psi} \quad (30)$$

Spherical coordinates (r, θ, ϕ) , $\psi = \psi(r, \theta)$

Then, Eq. (30) becomes

$$\frac{\partial^2 \psi}{\partial r^2} + \frac{1 - \mu^2}{r^2} \frac{\partial^2 \psi}{\partial \mu^2} + I(\psi) \frac{dl}{d\psi} = 0, \quad \mu \equiv \cos \theta \quad (31)$$

There exist separable solutions of the forms:

$$\psi = \frac{P(\mu)}{r^n} \quad (32)$$

$$I(\psi) = \alpha \psi^{1+1/n} \quad (33)$$

where α and n are parameters.

An axisymmetric NLFF equilibrium (2)

[Low & Lou, 1990]

The function $P(\mu)$ satisfies the nonlinear ODE

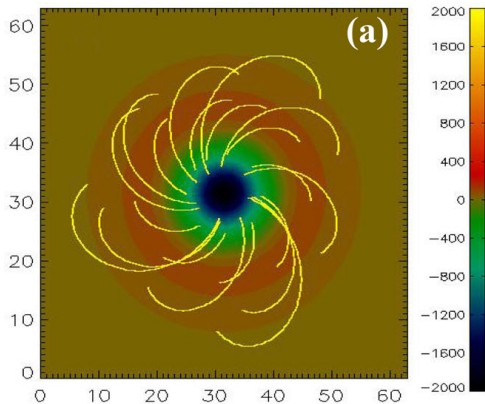
$$(1 - \mu^2) \frac{d^2 P}{d\mu^2} + n(n+1)P + \alpha^2 \frac{1+n}{n} P^{1+2/n} = 0. \quad (34)$$

To avoid a singularity of B_θ and B_ϕ at the origin:

$$P|_{\mu=\pm 1} = 0 \quad (35)$$

- The boundary value problem posed by (34) and (35) should be solved numerically to generate the sought NLFF fields.
- The resulting configurations are very popular for testing numerical algorithms for a 3D NLFFF modeling [e.g. Aschwanden & Malanushenko, 2013].

Low & Lou NLFF configuration



The 2D equilibrium in spherical coordinates shown is invariant in ϕ . The colour-coding corresponds to the vertical magnetic field strength in Gauss in the photosphere and a number of arbitrary selected magnetic field lines are shown in yellow. The distances on the axes are in pixel of the computational grid.

Outline

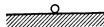
- MHD: Introduction
- Thermonuclear Fusion
- Equilibrium and Relaxation
- **Linear stability**
- Summary

Mechanical analogy of various types of equilibrium



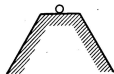
A

NO EQUILIBRIUM



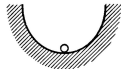
B

NEUTRALLY STABLE



C

(METASTABLE)
EQUILIBRIUM



D

STABLE EQUILIBRIUM



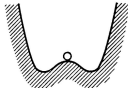
E

UNSTABLE EQUILIBRIUM



F

EQUILIBRIUM WITH LINEAR
STABILITY AND NONLINEAR
INSTABILITY



G

EQUILIBRIUM WITH
LINEAR INSTABILITY
AND NONLINEAR
STABILITY

The hydrodynamic Rayleigh-Taylor instability

If a heavy liquid is on top of a lighter one, it would tend to go down to the state “light on top”. The potential energy in the first state is higher than in the end state.

Indeed, consider two thin layers of different mass densities and compute the potential energy:

$$\text{State 1 : } W_p^1 = \rho_1 g h_1 + \rho_2 g h_2$$

$$\text{State 2 : } W_p^2 = \rho_2 g h_1 + \rho_1 g h_2$$

$$\delta W_p = W_p^1 - W_p^2 = g(\rho_1 - \rho_2)(h_1 - h_2)$$

If $h_1 > h_2$ and $\rho_1 > \rho_2$ it follows $\delta W > 0$ and the system is unstable.

The second state “light on top” has a lower potential energy.

Linear (exponential) stability

All the quantities of interest are linearized about their equilibrium values

$$\mathbf{g}(\mathbf{r}, t) = \mathbf{g}_0(\mathbf{r}) + \tilde{\mathbf{g}}_1(\mathbf{r}, t)$$

$\mathbf{g}_0(\mathbf{r})$: equilibrium

$\tilde{\mathbf{g}}_1(\mathbf{r}, t)$: first-order perturbation ($|\tilde{\mathbf{g}}_1/\mathbf{g}_0| \ll 1$)

General form of $\tilde{\mathbf{g}}_1$:

$$\tilde{\mathbf{g}}_1(\mathbf{r}, t) = \mathbf{g}(\mathbf{r})e^{-i(\omega t)}$$

$$\omega = \Re\omega + i\Im\omega$$

$$\text{If } \begin{cases} \Im\omega < 0 \rightarrow \text{damping} \rightarrow \text{stability} \\ \Im\omega > 0 \rightarrow \text{growth} \rightarrow \text{instability} \end{cases}$$

In case of instability: **growth rate** = $|\Im\omega|$

Linearized ideal MHD equations (1)

Static equilibrium:

$$\mathbf{j}_0 \times \mathbf{B}_0 = \nabla P_0 + \rho_0 \nabla \Phi, \quad (\mathbf{g} = -\nabla \Phi)$$

$$\mathbf{j}_0 = \nabla \times \mathbf{B}_0$$

$$\nabla \cdot \mathbf{B}_0 = 0$$

$$\mathbf{v}_0 = 0$$

Linearized equations:

$$\begin{aligned} \rho_0 \partial_t \mathbf{v}_1 &= -\nabla P_1 + (\nabla \times \mathbf{B}_1) \times \mathbf{B}_0 \\ &\quad + (\nabla \times \mathbf{B}_0) \times \mathbf{B}_1 - \rho_1 \nabla \Phi \end{aligned} \quad (36)$$

$$\partial_t \mathbf{B}_1 = \nabla \times (\mathbf{v}_1 \times \mathbf{B}_0), \quad \nabla \cdot \mathbf{B}_1 = 0 \quad (37)$$

$$\partial_t P_1 = -\mathbf{v}_1 \cdot \nabla P_0 - \gamma P_0 \nabla \cdot \mathbf{v}_1 \quad (38)$$

$$\partial_t \rho_1 = -\nabla \cdot (\rho_0 \mathbf{v}_1) \quad (39)$$

Linearized ideal MHD equations (2)

Displacement vector:

$$\tilde{\mathbf{v}}_1 = \frac{\partial \tilde{\boldsymbol{\xi}}}{\partial t} \quad (40)$$

Initial data (convenient):

$$\begin{aligned} \tilde{\boldsymbol{\xi}}(\mathbf{r}, 0) &= \tilde{\mathbf{B}}_1(\mathbf{r}, 0) = \tilde{\rho}_1(\mathbf{r}, 0) = \tilde{P}_1(\mathbf{r}, 0) = 0 \\ \frac{\partial \tilde{\boldsymbol{\xi}}(\mathbf{r}, 0)}{\partial t} &\equiv \tilde{\mathbf{v}}_1(\mathbf{r}, t) \neq 0 \end{aligned} \quad (41)$$

Integration of (37)-(39) gives $\tilde{\mathbf{B}}_1$, \tilde{P}_1 , $\tilde{\rho}_1$ in terms of $\tilde{\boldsymbol{\xi}}$:

$$\tilde{\mathbf{B}}_1 = \nabla \times (\tilde{\boldsymbol{\xi}} \times \mathbf{B}_0) \quad (42)$$

$$\tilde{P}_1 = -\tilde{\boldsymbol{\xi}} \cdot \nabla P_0 - \gamma P_0 \nabla \cdot \tilde{\boldsymbol{\xi}} \quad (43)$$

$$\tilde{\rho}_1 = -\nabla \cdot (\rho_0 \tilde{\boldsymbol{\xi}}) \quad (44)$$

Linearized ideal MHD equations (3)

Inserting the expressions for $\tilde{\mathbf{B}}_1$, \tilde{P}_1 , $\tilde{\rho}_1$ into the momentum equation (36) yields

$$\rho_0 \frac{\partial^2 \tilde{\boldsymbol{\xi}}}{\partial t^2} = \mathbf{F}(\tilde{\boldsymbol{\xi}}) \quad (45)$$

Force operator:

$$\begin{aligned} \mathbf{F}(\tilde{\boldsymbol{\xi}}) = & (\nabla \times \tilde{\mathbf{B}}_1) \times \mathbf{B}_0 + (\nabla \times \mathbf{B}_0) \times \tilde{\mathbf{B}}_1 \\ & + \nabla(\tilde{\boldsymbol{\xi}} \cdot \nabla P_0 + \gamma P_0 \nabla \cdot \tilde{\boldsymbol{\xi}}) + (\nabla \Phi) \nabla \cdot (\rho_0 \tilde{\boldsymbol{\xi}}) \end{aligned} \quad (46)$$

Equation (45) gives the time evolution of a perturbation applied at $t = 0$ with initial values $\tilde{\boldsymbol{\xi}}(\mathbf{r}, 0) = 0$, $\partial \tilde{\boldsymbol{\xi}} / \partial t = \tilde{\mathbf{v}}_1(\mathbf{r}, t)$ and appropriate boundary conditions.

(Henceforth the subscript 0 is dropped from the equilibrium quantities.)

Normal-mode formulation

Instead of solving the initial value problem it is more practical to consider the equivalent problem of determining the normal modes of the system. On account of linearity of the momentum equation (45) and stationarity of the equilibrium quantities we assume

$$\tilde{\xi}(\mathbf{r}, t) = \xi(\mathbf{r})e^{-i(\omega t)}.$$

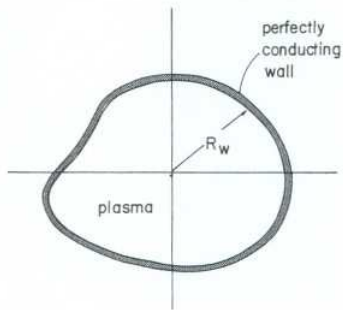
Eq. (45) then leads to the normal-mode formulation of the stability problem:

$$-\omega^2 \rho \xi = \mathbf{F}(\xi) \quad (47)$$

$$\begin{aligned} \mathbf{F}(\xi) = & (\nabla \times \mathbf{B}_1) \times \mathbf{B} + (\nabla \times \mathbf{B}) \times \mathbf{B}_1 \\ & + \nabla(\xi \cdot \nabla P + \gamma P \nabla \cdot \xi) + (\nabla \Phi) \nabla \cdot (\rho \xi) \end{aligned}$$

In this approach only appropriate **boundary conditions for ξ** are required. Eq. (47) can then be solved as an eigenvalue problem for the eigenvalues ω_i^2 and the eigenfunctions ξ_i .

Simplest boundary condition (internal modes)



The plasma extends out to a stationary, smooth, perfectly conducting wall, S_w on which

$$\mathbf{n} \cdot \boldsymbol{\xi}|_{S_w} = 0.$$

This guarantees that

$$\mathbf{n} \cdot \mathbf{B}_1|_{S_w} = \mathbf{n} \cdot \mathbf{v}_1|_{S_w} = 0$$

Properties of the force-operator \mathbf{F}

- \mathbf{F} is **symmetric (self adjoint)**:

$$\int \boldsymbol{\eta} \cdot \mathbf{F}(\boldsymbol{\xi}) d\mathbf{r} = \int \boldsymbol{\xi} \cdot \mathbf{F}(\boldsymbol{\eta}) d\mathbf{r} ,$$

where $\boldsymbol{\xi}$ and $\boldsymbol{\eta}$ two arbitrary displacement vectors satisfying the boundary conditions.

- Consequently, for any discrete normal mode the corresponding eigenvalue ω^2 is **real**.
- Any two nondegenerate discrete normal modes are **orthogonal**:

$$\int \rho \boldsymbol{\xi}_m \cdot \boldsymbol{\xi}_n = 0 .$$

The modes are orthogonal with weight function ρ .

The energy principle

Multiplying the equation of motion $\rho \partial^2 \tilde{\xi} / \partial t^2 = \mathbf{F}(\tilde{\xi})$ by $\dot{\tilde{\xi}}$ and making use of the symmetry of \mathbf{F} yields that **the perturbed energy is conserved**:

$$\frac{dH}{dt} = \frac{\partial}{\partial t} \left[\frac{1}{2} \int \rho \dot{\tilde{\xi}}^2 d\mathbf{r} - \frac{1}{2} \int \tilde{\xi} \cdot \mathbf{F}(\tilde{\xi}) d\mathbf{r} \right] = 0 . \quad (48)$$

Perturbed potential energy: $\delta W(\tilde{\xi}, \tilde{\xi}) \equiv -\frac{1}{2} \int \tilde{\xi} \cdot \mathbf{F}(\tilde{\xi}) d\mathbf{r}$

Kinetic energy: $K(\dot{\xi}, \dot{\xi}) = \frac{1}{2} \int \rho \dot{\xi}^2$

Using $\tilde{\xi}(\mathbf{r}, t) = \xi(\mathbf{r}) e^{-i(\omega t)}$, (48) becomes

$$\delta W(\xi, \xi) = -\omega^2 K(\dot{\xi}, \dot{\xi}). \quad (49)$$

Necessary and sufficient condition for stability

Statement (a): If for **all** allowable ξ (i.e. ξ bounded in energy and satisfying appropriate boundary conditions)

$$\delta W(\xi, \xi) \geq 0 \quad (50)$$

the system is stable.

Statement (b): If for **any** allowable ξ

$$\delta W(\xi, \xi) < 0 \quad (51)$$

the system is exponentially unstable.

If there is an allowable **trial function** able to make $\delta W < 0$ the system may decrease its potential energy following this path; that is the existence of such a function making $\delta W < 0$ is **sufficient for instability**.

Different forms of the energy integral

$$(1): \quad \delta W = \frac{1}{2} \int_{V_p} d\mathbf{r} \left\{ |\mathbf{B}_1|^2 + \gamma P |\nabla \cdot \boldsymbol{\xi}|^2 - \boldsymbol{\xi}^* \cdot \mathbf{j} \times \mathbf{B}_1 \right. \\ \left. + (\boldsymbol{\xi}_\perp \cdot \nabla P) \nabla \cdot \boldsymbol{\xi}_\perp^* - \nabla \cdot (\rho \boldsymbol{\xi}) (\boldsymbol{\xi}^* \cdot \nabla \Phi) \right\} \quad (52)$$

The subscript \perp, \parallel refer to the equilibrium field \mathbf{B} .

A general complex function $\boldsymbol{\xi}$ has been admitted in connection with possible complex Fourier representation.

$$(2): \quad \delta W = \frac{1}{2} \int d\mathbf{r} \left\{ \begin{array}{l} \text{Alfvén} \quad \text{fast magnetoacoustic} \\ |\mathbf{B}_{1\perp}|^2 + |\mathbf{B}_{1\parallel} - (\boldsymbol{\xi}_\perp \cdot \nabla P) \mathbf{b}/B|^2 \\ \text{acoustic} \quad \text{kink} \\ + \gamma P |\nabla \cdot \boldsymbol{\xi}|^2 - j_\parallel (\boldsymbol{\xi}_\perp^* \times \mathbf{b}) \cdot \mathbf{B}_1 \\ \text{flute} \quad \text{gravitational} \\ - 2(\boldsymbol{\xi}_\perp \cdot \nabla P) (\boldsymbol{\kappa} \cdot \boldsymbol{\xi}_\perp^*) - \nabla \cdot (\rho \boldsymbol{\xi}) (\boldsymbol{\xi}^* \cdot \nabla \Phi) \end{array} \right\} \quad (53)$$

$\mathbf{b} = \mathbf{B}/B$, $j_\parallel = \mathbf{j} \cdot \mathbf{b}$, \mathbf{B} - curvature : $\boldsymbol{\kappa} = \mathbf{b} \cdot \nabla \mathbf{b}$ ($\boldsymbol{\kappa} \cdot \mathbf{b} = 0$)

The intuitive form of δW

- The first three terms in (53) are **stabilizing** while the three last ones as indefinite in sign may be **destabilizing**.
- The acoustic term indicates that the most unstable perturbations (in the context of minimizing δW) are **incompressible**:

$$\nabla \cdot \boldsymbol{\xi} = 0 \quad (54)$$

Since the parallel displacement ξ_{\parallel} enters only in this term, one can minimize δW by choosing ξ_{\parallel} such that (54) is satisfied:

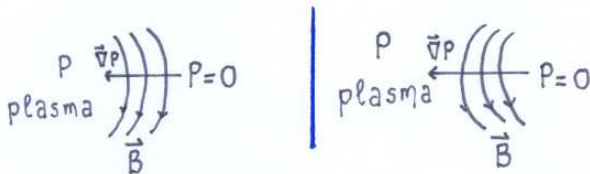
$$\mathbf{B} \cdot \nabla \left(\frac{\xi_{\parallel}}{B} \right) = -\nabla \cdot \boldsymbol{\xi}_{\perp} .$$

Pressure driven modes (flutes)

Possible destabilizing term:

$$- \int d\mathbf{r} (\boldsymbol{\xi}_{\perp} \cdot \nabla P) (\boldsymbol{\kappa} \cdot \boldsymbol{\xi}_{\perp}^*)$$

If $\boldsymbol{\kappa} \cdot \nabla P > 0$ ($\boldsymbol{\kappa} \parallel \boldsymbol{\xi}_{\perp}$), i.e if the curvature vector has a component along the pressure gradient, the mode is unstable.



The flute mode could be visualized roughly by saying that the centrifugal force plays the role of gravity and the stable situation is “light on top of heavy”.

Current driven modes (kinks)

Example [Tasso, 1979]: Force-free equilibrium

$$\mathbf{j} \times \mathbf{B} = \nabla P = \nabla \Phi = j_{\perp} = 0, \quad \mathbf{j} = \lambda \mathbf{B}$$

Then (52) becomes

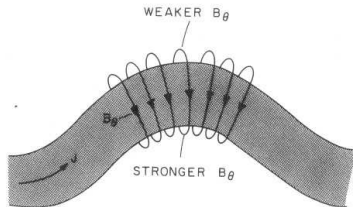
$$\delta W = \frac{1}{2} \int dr \left\{ \begin{array}{cc} \text{stabilizing} & \text{destabilizing} \\ |\mathbf{B}_1|^2 & - \xi^* \cdot (\mathbf{j} \times \mathbf{B}_1) \end{array} \right\}$$

It is possible to make $|\mathbf{B}_1|^2 = |\nabla \times (\xi \times \mathbf{B})|^2$ small, then the second term may overcome the first one. So, for stability one should try to prevent $|\mathbf{B}_1|^2$ from becoming too small. It turns out that the **magnetic shear**, $s = (1/r)dq/dr$, where q is the safety factor measuring the pitch of the magnetic field lines, tends to increase \mathbf{B}_1 in magnitude (over the plasma radius).

While in general current-driven unstable modes are **radially extended** depending on the current distribution, pressure driven modes are rather sensitive to the damping effect of magnetic shear and hence tend to be **radially localized**.

The kink instability

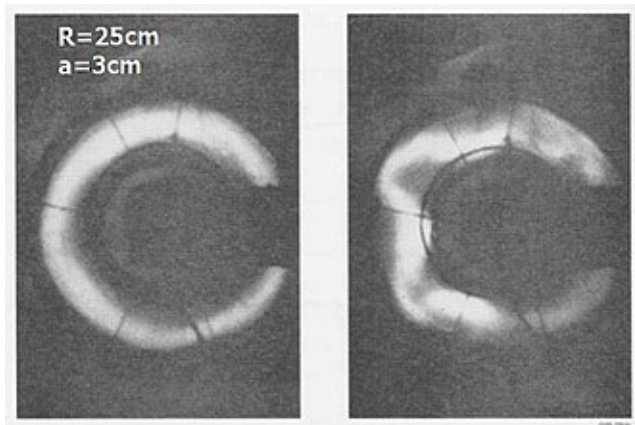
Destabilizing term: $-|\mathbf{j}|(\boldsymbol{\xi}_{\perp}^* \times \mathbf{b}) \cdot \mathbf{B}_1$



In a cylindrical plasma with axial equilibrium current (z-pinch) creating a purely azimuthal (poloidal) magnetic field, B_{θ} , a kink-like perturbation make the magnetic lines below closing together than those above. The resulting magnetic-pressure-gradient force increase the perturbation further.

The mode can be stabilized by applying an external magnetic field parallel to the current

Laboratory demonstration of the kink instability

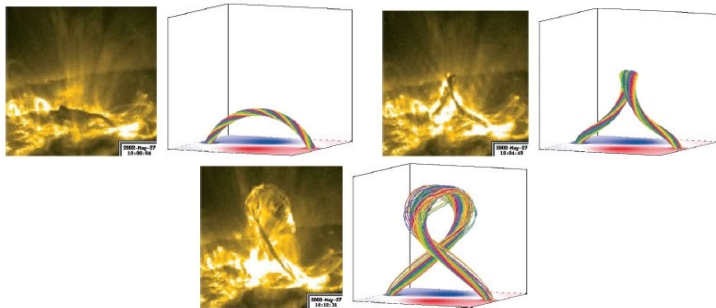


One of the earliest photos of the kink instability in action - the 3 by 25 cm pyrex tube at Aldermaston

[https://en.wikipedia.org/wiki/Kink_instability].

Kink instability at the Sun

Kinky flux: Ideal-MHD numerical simulations of twisted magnetic field lines on the solar surface show how the kink instability results in solar flares [Fan, 2005; Török & Kliem, 2005; Hanlon, 2005].



Images from the TRACE satellite showing the evolution of a filament eruption on the solar surface are well matched by numerical simulations of the magnetic field lines of a coronal loop [from Török & Kliem, 2005].

Summary (1)

- Magnetohydrodynamics (MHD), in the framework of which the plasma is treated as an electrically conducting fluid, can describe a broad range of laboratory and astrophysical plasmas.
- In particular, for high-temperature plasmas with negligible electrical resistivity, the ideal-MHD equations remain scale invariant in a huge range of spatial dimensions, densities and magnetic fields; high temperature plasmas are pertinent to the controlled thermonuclear fusion, a successful outcome of which would cover completely the globe's energy needs, and physical phenomena in the star's atmospheres as the Sun coronal mass ejections.
- The symmetric (2D) ideal MHD equilibria are governed by the Grad-Shafranov equation, a second-order, elliptic, quasilinear, PDE for the poloidal magnetic flux-function.

Summary (2)

- The Solovév solution of the GS equation has been employed extensively in tokamak studies; also, it is employed for modeling Sun physical phenomena.
- Of particular importance are force-free equilibria, having plasma currents parallel to the magnetic field, to describing relaxed states of the reversed-field pinch and spheromak and magnetic field configurations in the Sun atmosphere.
- The ideal-MHD linear stability is ruled by the Energy Principle, involving the potential energy of the perturbations. Because of the self-adjointness of the force-operator, this principle provides necessary and sufficient conditions for stability.
- Ideal MHD instabilities include pressure driven and current driven modes, i.e. macroscopic instabilities, evolving in a fast (Alfvénic) time scale. An example is the kink instability which should be controlled in laboratory fusion plasmas and it plays a role in the creation of Sun flares.

References (1)

- Albanese R., Blum J., De Barbieri O., 8th *Europhysics Conference on Computational Physics, Eibsee, 13-16 May 1986*, ECA 10D, 41 (1986).
- Alissandrakis C. E., *Astron. Astrophys.* **100**, 197 (1981).
- Arapoglou I, Throumoulopoulos G. N., Tasso H., *Phys. Lett. A* **377**, 310 (2013).
- Aschwanden M. J., Malanushenko A., *Sol. Phys.* **287**, 345 (2013).
- Bodin, H. A. B., 1984, in *Proceedings of the International Conference on Plasma Physics, Lausanne*, edited by M. Q. Tran and R. J. Verbeek (EEC, Brussels), Vol. I, p. 417.
- Bondeson A. G., Marklin Z. G., An H.H. et al., *Phys. Fluids* **24**, 1682 (1981).
- Chiu Y. T., Hilton H. H. *Astrophys. J* **212**, 873 (1978).
- Fan Y., *Astrophys. J.* **630**, 543 (2005).
- Finn, J. M., Mannheimer W. M., & Ott E. *Phys. Fluids* **24**, 1336 (1981).
- Freidberg J. P., *Ideal Magnetohydrodynamics*, Cambridge University Press, 2014.
- Goedbloed H. & Poedts S., *Principles of magnetohydrodynamics with applications to laboratory and astrophysical plasmas*, Cambridge University Press, 2004.
- Grad H., *Phys. Fluids* **10**, 137 (1967).
- Helander, P., *Rep. Progr. Phys.* **77**, 087001 (2024).

References (2)

- Linan L. et al., *Astronomy & Astrophysics* **681** A103 (1924).
- Low B. C., Lou Y. Q., *Astrophys. J.* **352**, 343 (1990).
- Poulipoulis G., Throumoulopoulos G. N., Konz C. et al, *Phys. Plasmas* **23**, 072507 (2016).
- Poulipoulis, Throumoulopoulos G. N., *AIP Advances*. **11**, 065231 (2021).
- Priest E. R., *Solar magnetohydrodynamics*, D. Reidel Publishing Company, 1982.
- Shafranov V. D., *Reviews of Plasma Physics* **2**, 103 (1966).
- Stix T. H., *Phys. Rev. Lett.* **30**, (1973).
- Tasso H., *Lectures on Plasma Physics*, Report IFUSP/P-181, LFP-8, Universidade de São Paulo, Instituto de Física, 1979. The document may be found via the EPAPS homepage (<http://www.aip.org/pubservs/epaps.html>) or from <ftp.aip.org> in the directory /epaps/. See the EPAPS homepage for more information.
- Taylor B. J., *Phys. Rev. Lett.* **33**, 1139 (1974).
- Török T & Kliem B., *Astrophys. J.* **630**, L97 (2005).
- Turner W. C., Goldenbaum G. C., Granneman E. H. A., *Phys. Fluids* **26**, 1965 (1983).
- Wesson J., *Tokamaks*, third edition, Clarendon Press-Oxford, 2004.
- Wiegelmann T., Sakurai T. *Living Reviews in Solar Physics* **18**, 1 (2021).
- Woltjer L., *Proc. Nat. Acad. Sci.* **44**, 489 (1958).
- Zakharov L. E. and Pletzer A., *Phys. Plasmas* **6**, 4693 (1999).